

Solvent Directed Templated Synthesis of Mono- and Di(Schiff Base) Complexes of Ni(II)¹

Y. Ding^{a,b}, F. Wang^b, Z. J. Ku^a, L. S. Wang^a, and Q. R. Wang^a

^a College of Chemistry and Materials Science, Xiaogan University, 432000 Xiaogan, China

^b Key Laboratory of Pesticide and Chemical Biology of Ministry of Education, College of Chemistry, Central China Normal University, 430079 Wuhan, P.R. China

e-mail: dy9802@126.com

Received June 8, 2008

Abstract—The mono- and binuclear complexes Ni(Salen) (I) and Ni₂(Salen)₂ (II) (H₂Salen = N,N'-bis(salicylidene)ethane-1,2-diamine), have been synthesized and structurally characterized by single-crystal X-ray diffraction studies. The X-ray structural analyses show that the metal center of complex I is mononuclear and tetra-coordinate with a distorted tetrahedron, whereas the metal-centered complex II is binuclear and pentacoordinate with rectangular pyramid geometries, respectively. The electrochemical studies evidenced for the mononuclear Ni(II) complex shows one quasireversible reduction potential at –0.80 V (*E*_{pc}) and the binuclear Ni(II) complex shows a reduction potential at –0.90 V (*E*_{pc}) in the cathodic region.

DOI: 10.1134/S107032840905008X

INTRODUCTION

Schiff bases play an important role in inorganic chemistry as they easily form stable complexes with most transition metal ions. The development in the field of bioinorganic chemistry has increased the interest in Schiff base complexes, since it has been recognized that many of these complexes may serve as models for biologically important species [1–5].

The literature on transition metal–Salen complexes is vast [6]. Salen derivatives and their metal complexes have been synthesized and characterized [7]. Many of these metal–Salen complexes have been used as potential catalysts for organic transformation of industrial importance [8]. In recent time, supramolecular chemistry has recognized Salen complexes because of their involvement in π – π stacking interactions among chelate rings and the associated aromatic rings [9]. The tetradentate di(Schiff base) ligands formed by the condensation of several diamines with salicylaldehyde or acetylacetone and their derivatives are well known for many years [10]. In this paper we report the solvent directed templated synthesis and structural characterization of mono- and di(Schiff base) Ni(II) complexes.

EXPERIMENTAL

All reagents were of analytical grade and used without further purification. The Schiff base (H₂Salen = N,N'-bis(salicylidene)ethane-1,2-diamine) was synthesized according to the literature method [6].

Synthesis of the complex Ni(Salen) (I). An equimolar mixture of nickel acetate and H₂Salen in methanol as solvent was stirred and kept at an appropriate temperature, and then allowed to stand for about one week, whereupon a yellow rectangular crystal was obtained, and recrystallized from DMF giving pale-yellow crystals for X-ray analysis.

Complex Ni₂(Salen)₂ (II). An equimolar mixture of nickel acetate and H₂Salen in the mixed solvent of DMF and 2-aminepyridine was stirred and kept at an appropriate temperature, and then allowed to stand for several weeks, whereupon a yellow block crystal was obtained, and recrystallized from DMF giving pale-yellow crystals for X-ray analysis.

Physical measure. Infrared spectra (400–4000 cm^{–1}) were measured on a Nicolet 380 FT-IR spectrophotometer (KBr pellet), and elemental analyses were carried out on a Vario elemental III (German) instrument. Cyclic voltammetric experiments were performed with an electrochemical analyzer (CH. Instrument 650c.). A standard three-electrode cell was used with a graphite-working electrode, a platinum auxiliary electrode, and a Ag/AgCl as reference electrode. The potential of this electrode was calibrated vs. SCE using the [Fe(C₅H₅)₂⁺]/[Fe(C₅H₅)₂] redox couple as an internal standard. All the experiments were performed in high-purity DMF and a pyridine solution with 0.1 M tetra-*n*-butyl ammonium chloride as supporting electrolyte.

X-ray data collection and structure refinement. Complex I: a pale-yellow crystal having an approximate dimension of 0.33 × 0.28 × 0.25 mm was used for data collection. Diffraction data for complex I were col-

¹ The article is published in the original.

Table 1. Crystallographic data of complexes **I** and **II**

Parameter	Value	
	complex I	complex II
Empirical formula	C ₁₆ H ₁₄ N ₂ NiO ₂	C ₃₂ H ₂₈ N ₄ Ni ₂ O ₄
<i>M</i>	325.00	650.00
Crystal system	Orthorhombic	Monoclinic
Space group	<i>Pbca</i>	<i>C2/c</i>
<i>a</i> , Å	7.4720(4)	26.639(2)
<i>b</i> , Å	13.8047(8)	6.9775(6)
<i>c</i> , Å	13.8047(8)	14.7094(12)
β, deg	90.00	97.5010(10)
<i>V</i> , Å ³	2692.0(3)	2710.7(4)
<i>Z</i>	8	4
ρ, g/cm ³	1.604	1.593
μ(MoK _α), mm ⁻¹	1.446	1.436
<i>F</i> (000)	1344	1344
Crystal size, mm	0.25 × 0.28 × 0.33	0.07 × 0.21 × 0.34
θ _{min} , θ _{max} , deg	2.95, 27.50	2.79, 27.50
Index ranges	-9 ≤ <i>h</i> ≤ 9 -17 ≤ <i>k</i> ≤ 17 -16 ≤ <i>l</i> ≤ 33	-34 ≤ <i>h</i> ≤ 32 -7 ≤ <i>k</i> ≤ 9 -16 ≤ <i>l</i> ≤ 19
Total data	16268	8437
Unique data	3087 (<i>R</i> _{int} = 0.0199)	3090 (<i>R</i> _{int} = 0.0229)
Observed data (<i>I</i> > 2σ(<i>I</i>))	2592	2607
<i>R</i> , <i>wR</i> ₂	0.0238, 0.0603	0.0243, 0.0531
GOOF	0.970	1.027
Largest diff. peak and hole, <i>e</i> Å ⁻³	0.231, -0.2226	0.394, -0.180

Table 2. Selected bond lengths (Å) and bond angles (deg) for the complexes **I** and **II**

Bond	<i>d</i> , Å	Bond	<i>d</i> , Å
I		II	
Ni(1)–N(1)	1.8454(13)	Ni(1)–N(1)	1.9650(13)
Ni(1)–O(1)	1.8455(11)	Ni(1)–O(1)	1.9412(10)
Ni(1)–O(2)	1.8519(11)	Ni(1)–O(2)	1.9115(11)
Ni(1)–N(2)	1.8503(13)	Ni(1)–N(2)	1.9484(13)
Angle	ω, deg	Angle	ω, deg
I		II	
O(2)Ni(1)O(1)	85.14(15)	O(2)Ni(1)O(1)	95.35(5)
O(1)Ni(1)N(2)	178.43(5)	O(2)Ni(1)N(2)	171.05(5)
O(2)Ni(1)N(2)	94.53(6)	O(1)Ni(1)N(2)	91.21(5)
O(1)Ni(1)N(1)	93.95(6)	O(2)Ni(1)N(1)	92.35(5)
O(2)Ni(1)N(1)	178.45(6)	O(1)Ni(1)N(1)	170.36(5)
N(2)Ni(1)N(1)	86.15(6)	N(2)Ni(1)N(1)	83.67(6)

lected at 295 K with a Siemens SMART-CCD diffractometer using graphite-monocromated, MoK $_{\alpha}$ radiation ($\lambda = 0.071073$ nm). A total of 16268 reflections were collected in the range of $2.95^{\circ} \leq 2\theta \leq 27.50^{\circ}$, 3087 reflections were independent ($R_{\text{int}} = 0.0199$), of which 2592 observed reflections with $I > 2\sigma(I)$ were used in the succeeding structure determination and refinements. The raw data were corrected, and the structure was solved using the SHELX-97 program. Non-hydrogen atoms were located by direct phase determination and subjected to anisotropic refinements. The full-matrix least-squares calculations on F^2 were applied to the final refinement. It converged at $R = 0.0238$ and

$$wR = 0.0603 \quad (w = 1/(\sigma^2(F_o^2) + (0.0609P)^2 + 1.3391P),$$

where $P = (F_o^2 + 2F_c^2)/3$. The residual peaks on the final difference Fourier map are 0.231 and $-0.226 \text{ e } \text{\AA}^{-3}$, respectively. The goodness-of-fit indicator (S) is 0.097, and $(\Delta/\sigma)_{\text{max}}$ is 0.04.

Complex **II**: a pale-yellow crystal of complex **II** having approximate dimension $0.34 \times 0.21 \times 0.07$ mm was used for data collection. Diffraction data for complex **II** were collected at 273 K with a Siemens SMART-CCD diffractometer using graphite-monocromated, MoK $_{\alpha}$ radiation ($\lambda = 0.071073$ nm). A total of 8437 reflections were collected in the range of $2.79^{\circ} \leq 2\theta \leq 27.50^{\circ}$, 3090 reflections were independent ($R_{\text{int}} = 0.0229$), of which 2607 observed reflections with $I > 2\sigma(I)$ were used in the succeeding structure determination and refinements. The raw data were corrected, and the structure was solved using the SHELX-97 program. Non-hydrogen atoms were located by direct phase determination and subjected to anisotropic refinements. The full-matrix least-squares calculations on F^2 were applied to the final refinement. It converged at $R =$

0.0243 and $wR = 0.0531$ ($w = 1/(\sigma^2(F_o^2) + (0.0243P)^2 + 0.8084P)$, where $P = (F_o^2 + 2F_c^2)/3$). The residual peaks on the final difference Fourier map are 0.394 and $-0.180 \text{ e } \text{\AA}^{-3}$, respectively. The goodness-of-fit indicator (S) is 1.027, and $(\Delta/\sigma)_{\text{max}}$ is 0.097. All crystallographic data and experimental details of the complexes are listed in Table 1. Selected bond lengths and bond angles are listed in Table 2.

Supplementary data have been deposited with the Cambridge Crystallographic Data Centre (no. 654304 for **I** and 654305 for **II**; deposit@ccdc.cam.ac.uk or www:http://www.ccdc.cam.ac.uk).

RESULTS AND DISCUSSION

An ORTEP view of neutral Ni(II) complex **I** with the atomic numbering scheme is shown in Fig. 1a. The metal center possesses a tetrahedrally distorted square planar geometry (torsion angle O(1)N(1)N(2)O(2) $-2.02(5)^{\circ}$) with N $_2$ O $_2$ donor atoms coordinating from the tetradenate Salen ligand, the sum of bond angles at the Ni(II) atom is 359.81° . The Ni(II) atom resides a little out by 0.001 Å of the N $_2$ O $_2$ plane. The structure comprises one five and two six-membered chelate rings. Both the six-membered metallocycles are practically coplanar with the N $_2$ O $_2$ coordination plane (dihedral angle 6.63°). The five-membered metallocycle deviates from the N $_2$ O $_2$ plane (torsion angle N(1)C(16)C(15)N(2) = -33.78°). The Ni–N and Ni–O distances and the selected angles are list in Table 2. As shown in Fig. 2a, the plane-to-plane distances and displacement angles of Cg2...Cg3, Cg3...Cg4 and Cg4...Cg5 are 3.3047(8), 3.8481(10) and 4.0700(11) Å and 6.63° , 9.09° , and 6.70° , showing strong π – π interac-

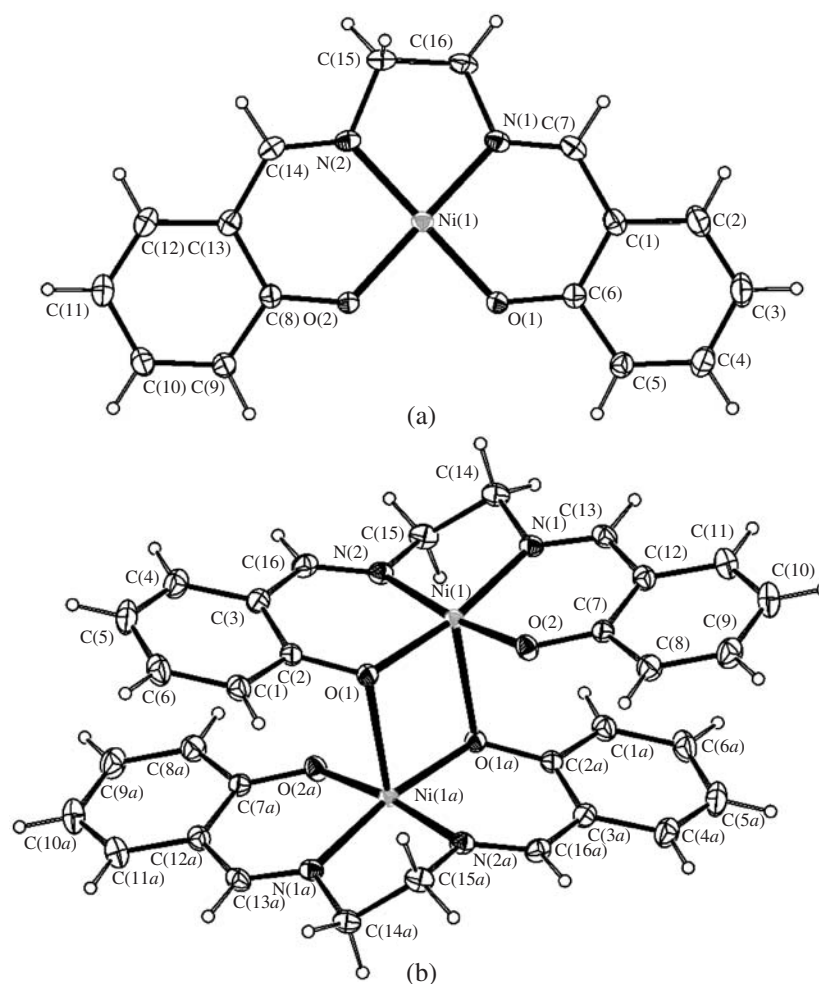


Fig. 1. ORTEP diagram of complex **I** (a) and **II** (b) with the atom numbering scheme.

tions, which are the factors that stabilized the crystal structure (*Cg2*, *Cg3*, *Cg4*, and *Cg5* are Ni(1)–O(1)/N(1), Ni(1)–O(2)/N(2), C(1)–C(6), and C(8)–C(13) centroids).

The molecular structure of complex **II** is shown in Fig. 1b, the asymmetric unit of the title compound, [Ni(Salen)₂], contains an Ni²⁺ cation, which is coordinated by two imine N atoms and by two phenolate O atoms of the Salen ligand, leading to a distorted square-planar conformation. When a secondary Ni–O interaction to the neighboring phenolate O atom is considered, two molecules are linked into a centrosymmetric dimer. Weak π – π interactions with a shortest interplanar distance of 3.704 Å help to stabilize the crystal structure.

The coordination sphere of the Ni(II) (NiN₂O₃) has a distorted square pyramidal geometry, which is bonded by two N atoms and three O atoms (including an oxo-bridge) from two Schiff base ligands. The equatorial atoms N(1), N(2), O(1), and O(2) about the nickel(II) atom are nearly coplanar with the nickel atom deviating by 0.063 Å from this plane. The oxo-bridge

atom (O(1a)) occupies the axial position. The Ni–O_{phenol} mean bonds of 1.9264 Å and the Ni–N_{imine} mean distances of 1.957 Å are unexceptional of similar Ni(II) systems. The Ni–O(1a) bridging bonds of 2.4106(11) Å, the Ni(1)O(1)Ni(1a) angle of 93.84(14)° and the Ni...Ni distance of 3.1946(4) Å are all consistent with the bi- μ -oxo-bridged nickel complex [11]. As shown in Fig. 2b, the plane-to-plane distances and displacement angles of *Cg4*...*Cg5* and *Cg5*...*Cg6* are 3.7035 and 4.0224 Å and 11.85°, 6.72°, respectively, showing weak π – π interactions, which are the factors that stabilized the crystal structure (*Cg4*, *Cg5* and *Cg6* are Ni(1)–O(2)/N(1), C(1)–C(6) and C(7)–C(12) centroids).

All of the relative bond angles and distances of complexes **I** and **II** are somewhat different, which conforms to the different solvents.

The electronic spectra of the two complexes were recorded in an acetonitrile solution. A broad band is observed near 800 nm, well separated from the second transition at ~510 nm for the both complexes. The third *d*–*d* band at a lower wavelength cannot be observed,

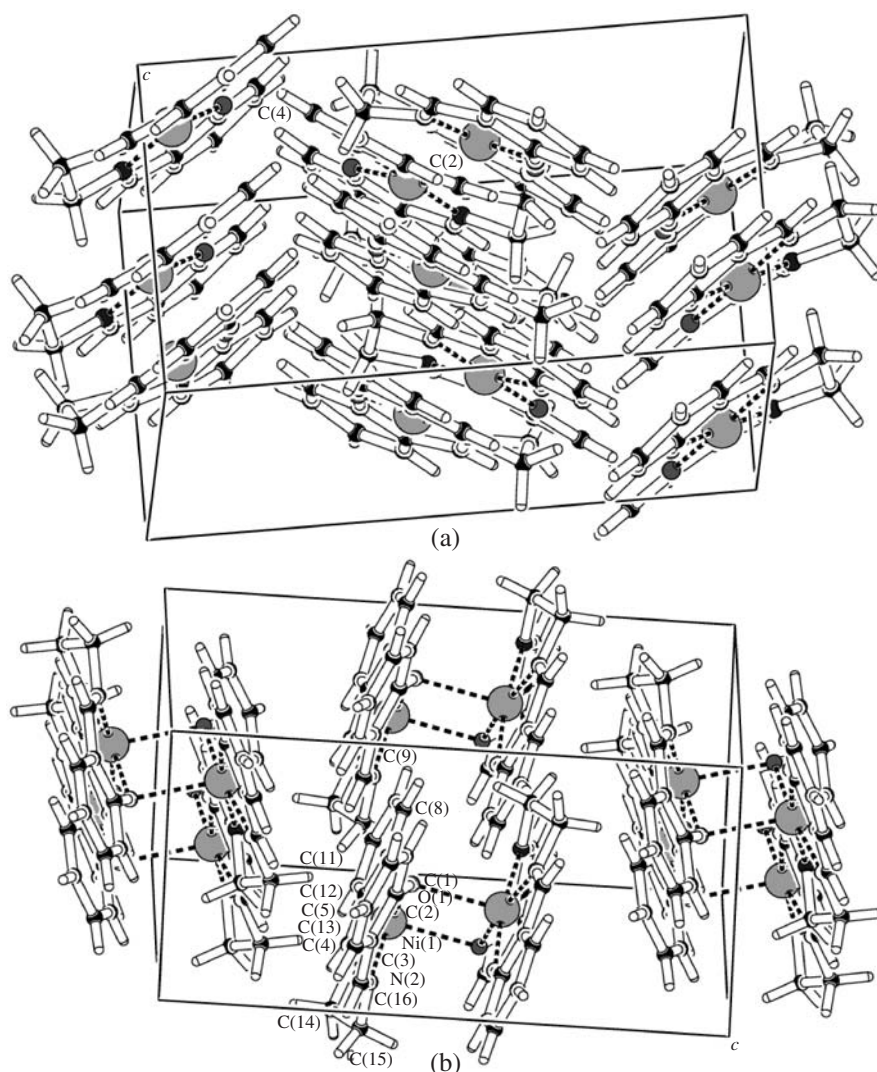


Fig. 2. Packing diagram showing π - π stacking interaction of complex **I** (a) and **II** (b).

because it is obscured by a strong charge-transfer transition in each case. The two absorption peaks are assigned to ${}^3T_{2g} \leftarrow {}^3A_{2g}$ and ${}^3T_{1g}(F) \leftarrow {}^3A_{2g}$ transitions. The calculated values of Dq lie in the ranges 1250–1260 cm^{-1} for all complexes and are in good agreement with literature values [12].

In the IR spectra of all the six complexes, the imine ($\text{C}=\text{N}$) stretch appears at $\sim 1650 \text{ cm}^{-1}$. The two NH_2 stretching modes are observed in the complexes of tetradentate ligands near 3340 and 3290 cm^{-1} as sharp bands (doublet) for the asymmetric and symmetric stretching vibrations, respectively.

The complexes show fluorescence. These are assigned as intraligand fluorescence (π - π^*). The spectroscopic data are given in Fig. 3 (DMF as solvent). Since the coplanarities of these complexes are decreased, the fluorescence emission lengths of them (475/6 and 496/2 nm for **I** and **II**, respectively) are

longer than those of the reported Schiff base complex [13–15].

The redox behavior of all the complexes were studied by using cyclic voltammetry in acetonitrile (0.1 M NEt_4ClO_4) in the potential range $\pm 1.6 \text{ V}$ by using a platinum auxiliary electrode and a Pt disc as a working electrode at ambient temperature (300 K) with no trace of decomposition as reflected in the smooth curve. The electrochemical activity of binuclear nickel(II) complex **II** shows that it can be oxidized by one electron to form Ni(III) at rather high potential of +0.965 V (vs. SCE), and the Ni(III) species is unstable and undergoes a rapid decomposition [15–18]. The peak separation ΔE between anodic and cathodic peaks is 1.446 V with $E_{pa} = 0.965 \text{ V}$ and $E_{pc} = -0.90 \text{ V}$, and $i_{pc}/i_{pa} \approx 1$.

Mononuclear Ni(II) complex **I** shows an irreversible oxidation wave in a positive potentials range at +0.80 V (E_{pa}). The binuclear Ni(II) complex shows two step single electron transfer processes in the potential range

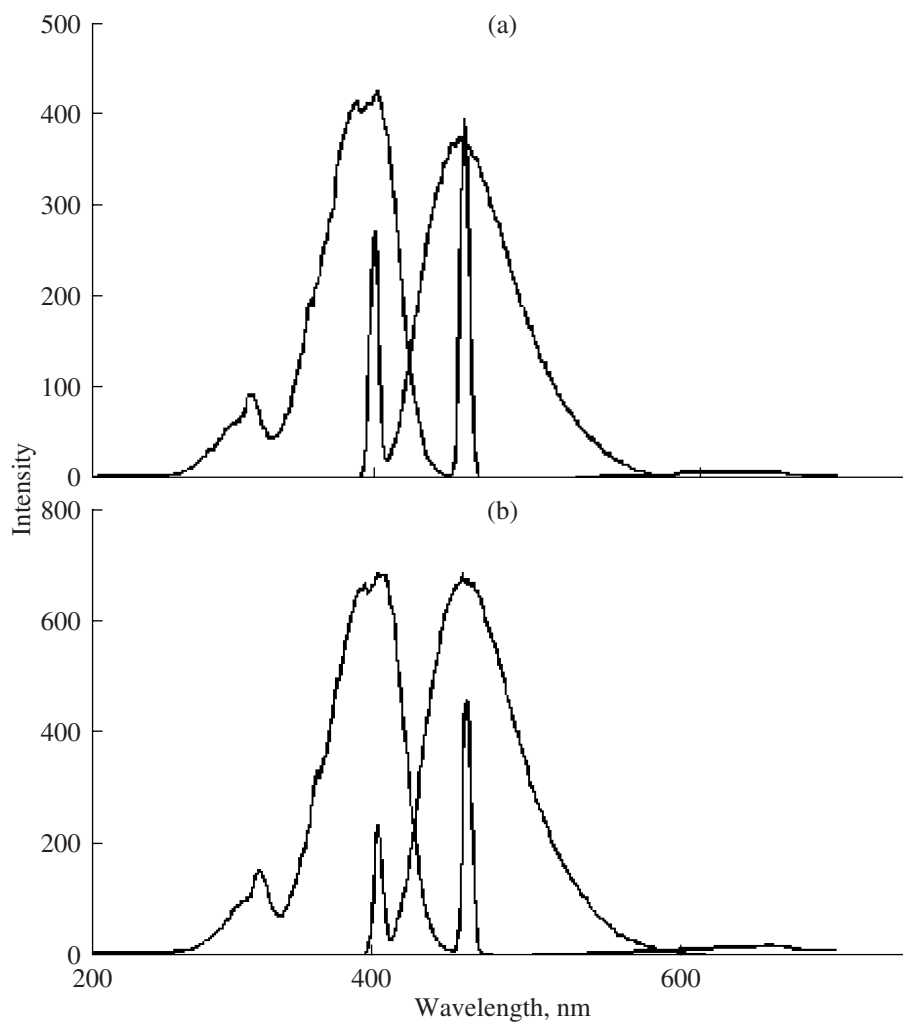


Fig. 3. The fluorescence spectrum of metal complex I (a) and II (b).

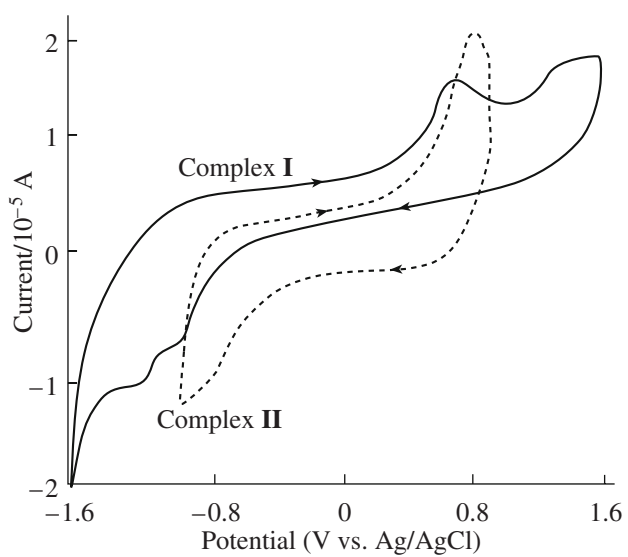
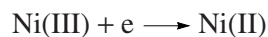


Fig. 4. Cyclic voltammograms of complexes I (a) and II (b).

+1.0 V (E_{pa}) which is found to be irreversible in nature, and cyclic voltammetry assigns quasireversibility to the electron step



and is shown in Fig. 4.

ACKNOWLEDGMENTS

This work was supported by the Program for Distinguished Young Scholars from Hubei Provincial Department of Education (project no. Q20082601).

REFERENCES

1. Chohan, Z.H. and Sheazi, S.K.A., *Synth. React. Inorg. Met.-Org. Chem.*, 1999, vol. 29, p. 105.
2. Rebouças, J.S., Cheu, E.L.S., Ware, C.J., et al., *Inorg. Chem.*, 2008, vol. 47, no. 17, p. 7894.
3. Liu, H.J., Miao, W.G., and Du, X.Z., *Langmuir*, 2007, vol. 23, no. 22, p. 11035.
4. Jayabalakrishnan, C. and Natarajan, K., *Synth. React. Inorg. Met.-Org. Chem.*, 2001, vol. 31, p. 983.
5. Hill, M.P., Carroll, E.C., Toney, M.D., et al., *J. Phys. Chem., B*, 2008, vol. 112, no. 18, p. 5867.
6. Lloret, F., Mollar, M., Faus, J., et al., *Inorg. Chim. Acta*, 1991, vol. 189, no. 2, p. 195.
7. Cozzi, P.G., *Chem. Soc. Rev.*, 2004, vol. 33, p. 410.
8. Atwood, D.A. and Harvey, M.J., *Chem. Rev.*, 2001, vol. 101, p. 37.
9. Canali, L. and Sherrington, D.C., *Chem. Soc. Rev.*, 1999, vol. 28, p. 85.
10. Tsuchida, E. and Oyaizu, K., *Coord. Chem. Rev.*, 2003, vol. 237, p. 213.
11. Liu, B. L., Li, F.A., and Mei, C. Z., *Chin. Chem. Rev.*, 2005, vol. 16, p. 13.
12. Drago, R. S., *Physical Methods in Chemistry*, Philadelphia: Saunders, 1977 (Ch. 11).
13. Ding, Y., Liu, Z.W., Zhang, Z.H., et al., *Acta Chim. Sin.*, 2007, vol. 65, no. 8, p. 688.
14. Wang, Y. and Yang, Z.Y., *J. Lumin.*, 2008, vol. 128, p. 373.
15. Chattopadhyay S., Drew, M.G.B., and Ghosh, A., *Inorg. Chim. Acta*, 2006, vol. 359, p. 4519.
16. Ding, Y., Zhang, Z.H., Hu, Z.Q., et al., *Chin. J. Inorg. Chem.*, 2006, vol. 22, no. 7, p. 1191.
17. Tümer, M., Ekinici, D., Tümer, F., et al., *Spectrochim. Acta*, Pt A, 2007, vol. 67, p. 916.
18. Chattopadhyay S., Drew, M.G.B., Ghosh, A., *Polyhedron*, 2007, vol. 26, p. 3513.